Ultrafast Photoinduced Electron Transfer between Tetramethylrhodamine and Guanosine in Aqueous Solution

ARTICLE *in* THE JOURNAL OF PHYSICAL CHEMISTRY B · MAY 2011

Impact Factor: 3.3 · DOI: 10.1021/jp200455b · Source: PubMed

4 AUTHORS, INCLUDING:

Anchi Yu
Renmin University of China
47 PUBLICATIONS **540** CITATIONS

SEE PROFILE

THE JOURNAL OF PHYSICAL CHEMISTRY B

ARTICLE

pubs.acs.org/JPCB

Ultrafast Photoinduced Electron Transfer between Tetramethylrhodamine and Guanosine in Aqueous Solution

Xun Li,[†] Ruixue Zhu,[‡] Anchi Yu,*[,‡] and Xin Sheng Zhao*[,†]

[†]Beijing National Laboratory for Molecular Sciences, State Key Laboratory for Structural Chemistry of Unstable and Stable Species, Department of Chemical Biology, College of Chemistry and Molecular Engineering, and Biodynamic Optical Imaging Center, Peking University, Beijing 100871, People's Republic of China

[‡]Department of Chemistry, Renmin University of China, Beijing 100872, People's Republic of China

Supporting Information

ABSTRACT: Photoinduced electron transfer based fluorescence correlation spectroscopy (PET-FCS) is a powerful tool to study biomolecular processes. However, some questions remain as to how to correctly interpret the PET-FCS data. In this work, we studied the PET process between tetramethylrhodamine and guanosine by means of femtosecond transient absorption spectroscopy. We derived that the charge separation rate is $4.1 \times 10^9\ s^{-1}$ and the charge recombination rate is $5.2 \times 10^{10}\ s^{-1}$ for the current system, supporting the three-state model and the interpretation on PET-FCS experiments given by Qu et al. (*J. Phys Chem. B*, **2010**, *114*, 8235). At the limit that both the charge separation and recombination rates are much faster than the process that PET-FCS reveals, the three-state model can be simplified to an equivalent two-state model with a dark state whose brightness is nonzero. We propose ways to obtain the brightness of the dark state with additional experiments, which is necessary for a PET-FCS study.

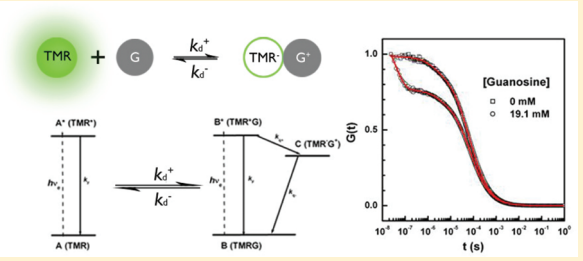

INTRODUCTION

The development of innovative fluorescence-based techniques to probe biomolecular interaction and dynamics is one of the major interests in biophysical chemistry.[1−9] The technique of fluorescence resonance energy transfer (FRET) is a widely used sensitive tool in biochemical and biophysical studies.[8−14] However, FRET has its own limitations. First, it requires site-specific labeling of two extrinsic chromophores. Second, on the basis of long-range dipole−dipole interaction its characteristic distance (ranging from 2 to 8 nm) is too long to probe subtle spatial changes. In contrast, photoinduced electron transfer (PET) requires a contact between the fluorophore and quencher at a subnanometer scale,[15−28] that makes PET an elegant alternation to the conventional FRET method. Until now, many fluorophores such as 2-aminopurine,[29−32] pyrene,[33−36] coumarin,[37] rhodamine,[2,3] oxazine,[38−45] fluorescein,[46,47] and bodipy-FL[48,49] have been reported to have PET interaction with a nucleobase, usually guanosine. Depending on the reduction potential of the fluorophore used, the efficient PET can occur between the first excited singlet state of the fluorophore and the ground state of guanosine.[17,20,37] Many researchers have proposed two different mechanisms, so-called "static" and "dynamic" quenching, for the deactivation of the excited fluorophore.[27,30,37] However, Zewail et al. has pointed out that this distinction depends on the actual time scale of the experimental methods.[32]

Tetramethylrhodamine (TMR) has been an important fluorophore to label biomolecules, such as the fluorescent antibody and avidin derivatives used in immunochemistry.[21,50−55] It is also a good candidate for PET.[40,56,57] Among the four nucleotides, guanosine is the one that has prominent PET quenching on TMR,[57] so that the TMR-guanosine pair could be used to probe the dynamic process involving DNA or RNA. Recently, Qu et al. have employed TMR as an electron acceptor to measure the rates on forward and reverse diffusions of intramolecular collision in unstructured overhang oligonucleotides with fluorescence correlation spectroscopy (FCS).[58] According to the standard two-state model,[45] the PET-FCS curve reflects the relaxation between an open fluorescent state and a closed nonfluorescent state, which is due to the formation of the charge separation state. However, Qu et al. found that the equilibrium constant obtained from their PET-FCS data through the standard two-state model is not identical to that obtained from the ensemble static fluorescence measurement.[58] On the basis of the experimental facts, they suggested a three-state model for the PET phenomenon, in which the closed state is composed of a fluorescent state and a nonfluorescent charge separation state. In addition, they argued that the lifetime of the closed state in the PET-FCS experiment should be the lifetime of the collision encounter instead of the charge separation state in the collision encounter, as they believed that the lifetime of the charge separation state in the collision encounter should be much shorter.

Received: January 16, 2011
Revised: March 30, 2011
Published: April 14, 2011

Since the actual picture of the PET process in a fluorophore-quencher collision is very basic and important in the understanding and interpretation of experimental observations, in this work we investigated the PET kinetics between TMR and guanosine in aqueous solution by carrying out femtosecond transient absorption measurements. We studied the decay of the first excited electronic state and the recovery of the ground electronic state of TMR in the presence of guanosine, so that we were able to derive the charge separation and recombination rates. We obtained that the charge separation rate is $4.1 \times 10^9\ s^{-1}$ and the charge recombination rate is $5.2 \times 10^{10}\ s^{-1}$. The data from the femtosecond transient spectroscopy are consistent with the data from the FCS and ensemble static fluorescence measurements, supporting the model and the interpretation on PET-FCS experiments given by Qu et al.[58] At the limit that both the charge separation and recombination rates are much faster than the process that PET-FCS reveals, the three-state model can be simplified to an equivalent two-state model with a dark state whose brightness is nonzero. We propose ways to obtain the brightness of the dark state with additional experiments, which is necessary for a PET-FCS study.

EXPERIMENTAL SECTION

Materials. Tetramethylrhodamine (TMR) and deoxy-guanosine were purchased from Sigma, U.S. and used as received. One × TE buffer (pH = 8.0) was diluted from 20 × TE (Molecular Probes, USA). Ultrapure water (18.2 MΩ•cm^{-2}) was obtained through either a PALL or a Milli-Q water purification system.

Femtosecond Transient Absorption Measurements. We used an amplified Ti:sapphire laser system (Spitfire, Spectra Physics, USA), which generates about 100 fs laser pulses at 840 nm with a repetition rate of 1 kHz and an average power of around 1.0 W. These fundamental pulses were used to pump an optical parametric amplifier (OPA) as well as to generate the white light continuum. The OPA pulses were about 100 fs and could be tuned from 450 to 700 nm. The white light continuum was generated in a spinning fused-silica disk with the 840 nm pump pulse and its spectrum covers the range of 420 to 750 nm. The OPA output was used as the pump, and the white light continuum was used as the probe. The timing between the pump and probe was controlled using a motorized translation stage (M-ILS250CC, Newport, USA). The pump and probe beams were noncollinearly focused into the sample cell using two achromatic lenses (300 mm focal length for the pump and 100 mm focal length for the probe, respectively). At the sample position, the average powers were about 0.5 mW for the pump and around 10 μW for the white light continuum probe. The signals were collected by a photomultiplier tube (R955, Hamamatsu, Japan) which was attached to an output port of a monochromator (SP2358, ARC, USA) and sent to a lock-in amplifier (SR850, SRS, USA) where it was synchronized by an optical chopper (75160, Newport, USA). The chopped frequency was 160 Hz. The polarization of the pump was set at 54.7° with respect to the polarization of the probe to get rid of the molecular reorientation effect. The time resolution of this apparatus was estimated to be about 150 fs through the cross-correlation between the pump and probe pulses in buffer solution.

Fluorescence Correlation Spectroscopy (FCS) Measurements. FCS measurements were conducted on a previously reported home-built dual-channel fluorescence microscope equipped with a CW Ya-Ge laser (532 nm) (SUW Tech., China) as the excitation source.[58−60] The laser beam was collimated and focused into the sample solution through an oil-immersion objective (100×, NA 1.4, Nikon, Japan) by a dichroic beam splitter (Cy3, Chroma Technology, USA). The emitted fluorescence was collected by the same objective, passed through appropriate filters (LP03−532RU, Semrock, USA) and 650−1100 nm holophote (Daheng, China), and focused through a 30-μm-diameter pinhole. The fluorescence photons were divided into two channels by a nonpolarizing 50/50 splitter (XF121, Omegafilters, USA), then focused onto two avalanche photodiodes (APD, SPCM-AQR-14, Perkin-Elmer, USA). The signals of the two APDs were recorded in the cross correlation mode using a computer implemented correlator (Flex02−12D, www.correlator.com, China). The temperature in the FCS experiments was controlled by a THMS600 temperature controller (Linkam, UK).

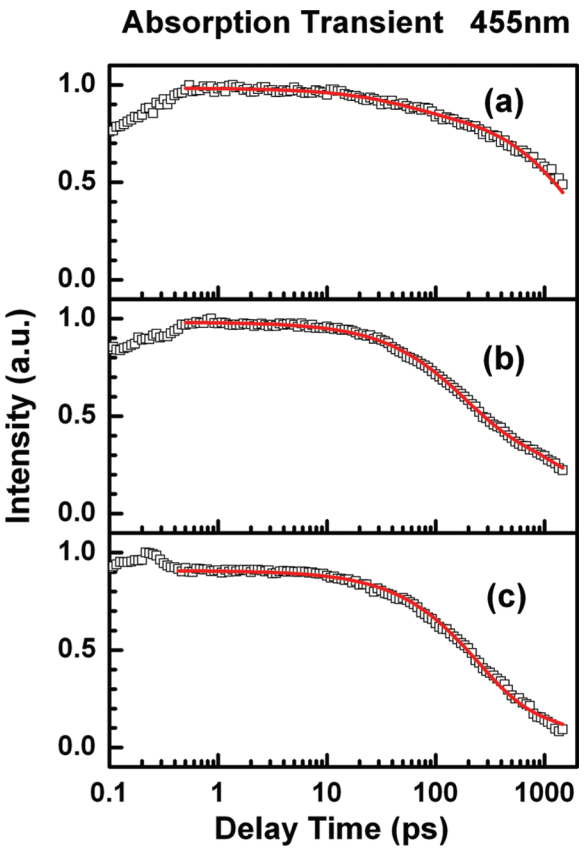

Figure 1. Magic-angle femtosecond pump−probe transients of TMR alone (a), TMR in 19.1 mM (b), and TMR in1.00 M (c) guanosine in 1 × TE buffer. Pump: 530 nm, probe: 445 nm.

Static Absorption and Fluorescence Measurements. Static absorption spectra were recorded by a commercial UV−vis spectrometer (U3100, Hitachi, Japan or Cary 50, Varian, Australia). Static fluorescence spectra were recorded on a Reinishaw 1000 microscopic spectrometer (UK) with a 514 nm argon ion laser (MG, USA). To record the weak fluorescence, a CCD detector (Spec10:400B, PI, USA) and laser excitation were also employed.

In all of the ultrafast measurements, the concentration of TMR was adjusted to have about 0.1 OD at its absorption maxima in a 1 mm path length sample cell. To keep the TMR solution fresh, a homemade magnet stirring bar was placed inside the sample cell and rotated by an external magnet motor. The static absorption spectra of the sample were measured before and after each ultrafast

Table 1. Excited-State Decay Parameters for TMR in Guanosine (G) Solutions[a]

	a_0	τ_0 (ps)[b]	a_2	τ_2 (ps)	χ^2
TMR+19.1 mM G	0.46	2200	0.54	164	1.05
TMR+1.00 M G	0.25	2200	0.75	230	1.06
	(0.20)	(2200)	(0.80)	(218)	(1.07)

[a] Data shown in the parentheses are obtained from the fs-fluorescence up-conversion measurements. [b] Fixed to match the lifetime obtained by the TCSPC measurements.

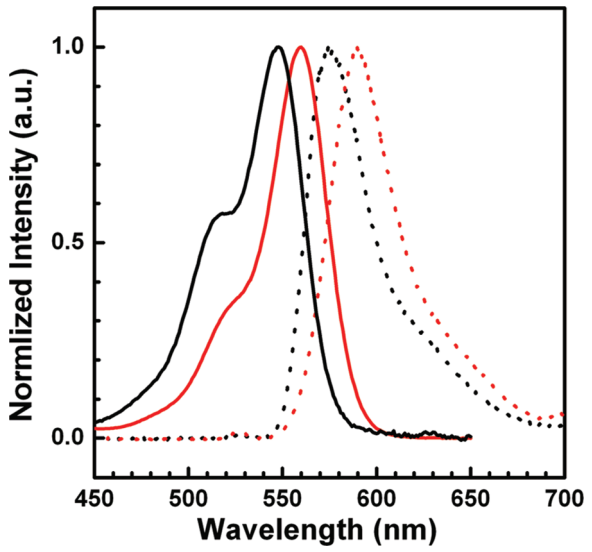

Figure 2. Normalized static absorption (solid line) and fluorescence (dot line) spectra of TMR without (black line) and with 1.00 M guanosine (red line) in 1 × TE buffer.

measurement to check the sample's quality and stability. The data were disregarded when the sample degradation was larger than 5%.

RESULTS AND DISCUSSION

Excited-State Decay of TMR. Figure 1 shows the decay of the first excited electronic state of TMR alone and in guanosine solutions, monitored through the transient absorption of $S_1 \rightarrow S_n$ transition[61] after TMR was excited into its first excited electronic state. The transient absorption of TMR without guanosine can be fitted by two exponential decays with the time constant (amplitude) of 2200 ps (0.89) and 50 ps (0.11), respectively. The 2200 ps lifetime is consistent with the lifetime of TMR alone in aqueous solution measured by time-correlated single photon counting technique (TCSPC, Figure S1 of the Supporting Information, SI) and in literatures.[21,40] Its fast component is most likely due to the interaction between TMR molecules, because the amplitude reduced with the decrease of the TMR concentration. However, we were unable to totally get rid of it, since the transient absorption measurement required rather high sample concentration. The transients of TMR with guanosine can also be fitted by two exponential decays, and the fitting parameters are listed in Table 1. The lifetime of the fast component (~200 ps) in the presence of guanosine is not the same as that of TMR alone (50 ps). More importantly, within the experimental error the lifetime and the amplitude in the presence

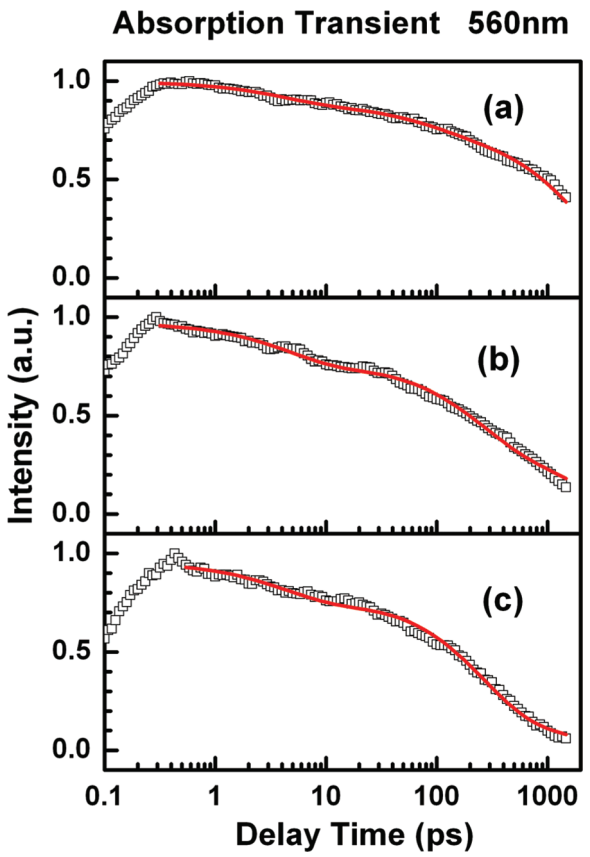

Figure 3. Magic-angle femtosecond pump−probe transients of TMR alone (a), TMR in 19.1 mM (b), and TMR in 1.00 M (c) guanosine in 1 × TE buffer. Pump: 530 nm, probe: 560 nm.

of guanosine did not vary with the variation of the TMR concentration. To confirm that the measured decays in the transient absorption were associated with the initially populated first excited state of TMR, we also performed femtosecond fluorescence up-conversion measurement on TMR in 1.00 M guanosine solution (Figure S2 of the SI). The up-conversion measurement gave a consistent result (Table 1).

It is seen from Table 1 that the lifetime of the fast component in the presence of guanosine did not vary with the guanosine concentration, but its amplitude did (also see Table S1 of the SI). This is a well-known behavior[32] and indicates the formation of a ground-state complex between TMR and guanosine. Thus, the ~200 ps decay component reflects the excited-state lifetime of the TMR-guanosine complex, while the 2200 ps decay component is the excited-state lifetime of free TMR. The evidence of the ground-state complex of TMR and guanosine can also be revealed through its static absorption and fluorescence spectra.[21,28,40,43] Figure 2 displays the normalized static absorption and fluorescence spectra of TMR with and without 1.00 M guanosine in aqueous solution. Obviously, the absorption and fluorescence emission maxima of TMR in 1.00 M guanosine are both red-shifted about 15 nm, which indicates the formation of ground-state complex between TMR and guanosine.

Ground-State Recovery of TMR. Figure 3 displays the recovery of the ground-state transient of TMR alone and in guanosine solutions, monitored through its ground-state transition ($S_0 \rightarrow S_1$)[61] after TMR was excited into its first excited electronic state. Three exponential components are required to fit the transient of TMR

Table 2. Ground-State Recovery Parameters for TMR in Guanosine (G) Solutions

	a_0	τ_0 (ps)[a]	a_1	τ_1 (ps)	a_2	τ_2 (ps)	τ_3 (ps)	χ^2
TMR+19.1 mM G	0.35	2200	0.23	4.6	0.42	231	17.5	1.08
TMR+1.00 M G	0.15	2200	0.22	4.3	0.63	258	20.5	1.06

[a] Fixed to match the lifetime obtained by the TCSPC measurements.

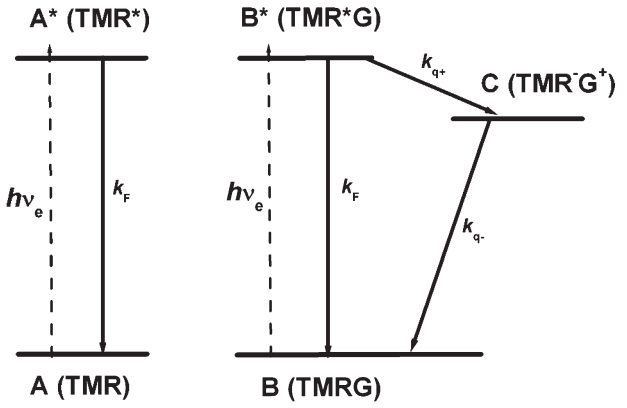

Figure 4. The dynamic model for the radiative and nonradiative (PET) pathways of the excited TMR.

alone, and the time constants (amplitudes) are 4.0 ps (0.12), 80 ps (0.13), and 2200 ps (0.75), respectively. The source of the 80 ps component in the ground-state recovery is the same as the 50 ps component in the exited-state decay, the 4.0 ps component is attributed to the solvent solvation time, and the 2200 ps component is the lifetime of the first excited electronic state of TMR. The transient absorption spectra on the ground-state recovery of TMR in 19.1 mM and 1.00 M guanosine solutions have to be fitted by more exponential terms, and the fitting parameters are shown in Table 2.

The transient absorption dynamics of the excited-state transition ($S_1 \rightarrow S_n$) and the ground-state transition ($S_0 \rightarrow S_1$) of TMR provide us with different information. For the PET scheme displayed in Figure 4, it is easy to derive that the $S_1 \rightarrow S_n$ absorption monitors the excited-state depopulation,

$$S_1(t) = S_{1,0}\exp(-(k_F + k_{q+})t) \quad (1)$$

where $S_{1,0}$ is the initial population of the excited-state immediately after the pump pulse arrives, k_F is the radiative fluorescence rate, and k_{q+} is the charge separation rate. Because we were unable to prepare a completely quenched TMR by guanosine, we have to add one more term in eq 1 to take the contribution from the free TMR into account. With the parameters listed in Table 1, we derive that $k_{q+} = (4.4 \pm 0.6) \times 10^9\ s^{-1}$ and $k_F = (4.5 \pm 0.2) \times 10^8\ s^{-1}$, respectively. While the $S_0 \rightarrow S_1$ transition allows us to follow the ground-state repopulation,

$$S_{0,0} - S_0(t) = \frac{(k_F - k_{q-})S_{1,0}}{(k_F + k_{q+} - k_{q-})}\exp(-(k_F + k_{q+})t) + \frac{k_{q+}S_{1,0}}{(k_F + k_{q+} - k_{q-})}\exp(-k_{q-}t) \quad (2)$$

where $S_{0,0}$ is the initial population in the ground-state before the pump pulse arrives, and k_{q-} is the charge recombination rate. Because we were unable to prepare a completely quenched TMR by guanosine and because of the solvent solvation effect on the kinetics of the ground-state recovery, we have to add two more terms in eq 2 to fit the data of the ground-state recovery,

$$S_{0,0} - S_0(t) = a_0\exp(-t/\tau_0) + a_1\exp(-t/\tau_1) + a_2\left(\exp(-t/\tau_2) + \frac{\tau_3(\tau_0 - \tau_2)}{\tau_2(\tau_3 - \tau_0)}\exp(-t/\tau_3)\right) \quad (3)$$

where τ_0 is the fluorescence lifetime of TMR without guanosine, τ_1 is the solvent solvation time, τ_2 is the fluorescence lifetime of TMR with guanosine, τ_3 is the lifetime of the charge separation state, and a_{0-2} are the amplitudes of each component. Figure 3 shows the fits with all fitting parameters listed in Table 2. With the parameters listed in Table 2, we derive that $k_{q+} = (3.7 \pm 0.6) \times 10^9\ s^{-1}$, $k_{q-} = (5.2 \pm 1.0) \times 10^{10}\ s^{-1}$, and $k_F = (4.5 \pm 0.2) \times 10^8\ s^{-1}$, respectively. Combining the data from both the excited-state decay and the ground-state recovery of TMR, we obtain that $k_{q+} = (4.1 \pm 0.8) \times 10^9\ s^{-1}$, $k_{q-} = (5.2 \pm 1.0) \times 10^{10}\ s^{-1}$, and $k_F = (4.5 \pm 0.2) \times 10^8\ s^{-1}$, respectively.

In addition, according to the PET scheme shown in Figure 4, the relative brightness of the complex of TMR and guanosine with respect to TMR alone is as follows:

$$Q = \frac{k_F}{k_F + k_{q+}} = \frac{\tau_2}{\tau_0} \quad (4)$$

With the fitting parameters shown in Tables 1 and 2, we calculate that $Q = 0.10 \pm 0.02$.

Among amino acid, tryptophan is the one that causes the most obvious fluorescence quenching of TMR (Figure S3 of the SI). We carried out parallel femtosecond transient experiments by replacing guanosine with tryptophan, and similar results were observed in the dynamics except that the decay rates are faster (Figures S4 and S5 of the SI).

FCS and Ensemble Static Fluorescence Measurements of TMR. If we do not differentiate the fluorescence and nonfluorescence states in the complex of TMR and guanosine but consider them together, then the three-state model in the PET-FCS measurement provided by Qu et al.[58] can be simplified to an equivalent two-state model (Figure 4),

$$A \underset{k_{d-}}{\overset{k_{d+}}{\rightleftarrows}} B \quad (5)$$

where state B is the collision complex composed of the fluorescent and nonfluorescent states, so that it has a nonzero relative brightness Q, and k_{d+} and k_{d-} are the forward and reverse diffusion rate constants. This simplification holds at the limit of k_F, k_{q+}, $k_{q-} \gg k_{d+}$, k_{d-}, which is true in current situation. The equilibrium constant is as follows:

$$K_d = \frac{k_{d+}}{k_{d-}} = \frac{C_B}{C_A} \quad (6)$$

where C_A and C_B are the concentrations of states A and B.

The relative brightness of state B (Q) and the equilibrium constant (K_d) can be obtained through the PET-FCS and ensemble static fluorescence measurements according to the model of Qu et al.[58] We performed the PET-FCS of TMR in 19.1 mM guanosine (Figure 5) and the ensemble static fluorescence measurements of TMR in guanosine of different concentrations (Figure 6). A thorough study on the quencher concentration dependence of the PET-FCS and the ensemble static fluorescence properties has been reported previously, and the reason for the nonlinearity of the Stern−Volmer-plot in

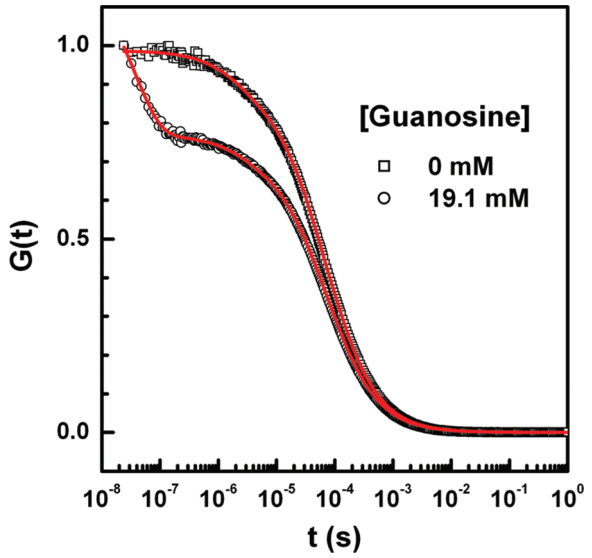

Figure 5. FCS curves of TMR with and without 19.1 mM guanosine in 1 × TE buffer.

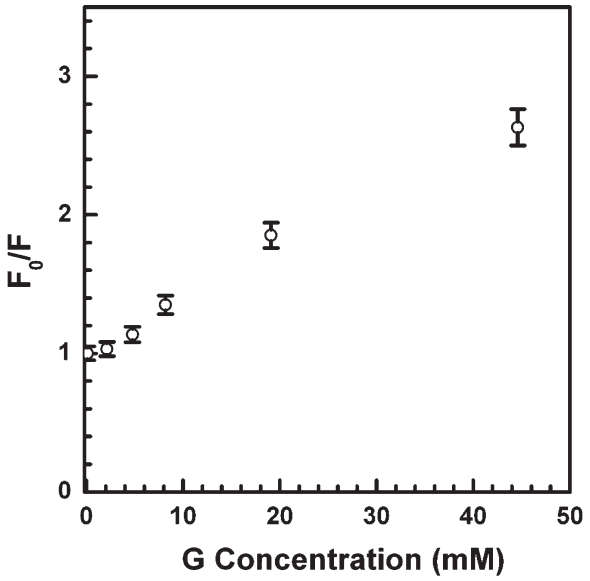

Figure 6. Static bimolecular Stern−Volmer plot of TMR in the presence of guanosine in 1 × TE buffer.

Figure 6 has also been discussed.[45] Our goal here is to make a comparison among the transient absorption spectroscopy, PET-FCS, and ensemble static fluorescence spectroscopy at a most sensitive condition (a quencher concentration that makes $K_d \approx 1$). Therefore, we skip the discussion on those properties that have been discussed and merely take the data to carry out following calculations. The PET-FCS curve could be fitted by the following:[58]

$$G(t) = G_D(t) \times \left(1 + \alpha \exp\left(-\frac{t}{\tau}\right)\right) \quad (7)$$

where $G_D(t)$ is the diffusion term and the following:

$$\tau = \frac{1}{k_{d+} + k_{d-}} \quad (8)$$

$$\alpha = \frac{(1-Q)^2 K_d}{(1+K_d Q)^2} \quad (9)$$

The experimental PET-FCS curve was fitted with two exponential decays. One component represents the triplet-singlet transition of TMR. When we controlled the laser power at around 50 μW, the pre-exponential amplitude of the triplet-singlet component is less than 0.05. The other component comes from the reaction of eq 5. From the ensemble static fluorescence measurement, we obtained the ratio (R) of fluorescent intensity of TMR in guanosine (F) over that without guanosine (F_0):[58]

$$R = \frac{F}{F_0} = \frac{C_A + QC_B}{C_0} \quad (10)$$

where $C_A + C_B = C_0$.

Combining the FCS and ensemble static fluorescence data, we have,[58]

$$Q = R - \frac{\alpha R^2}{1-R} \quad (11)$$

$$K_d = \frac{1-R}{R-Q} \quad (12)$$

For TMR in 19.1 mM guanosine, the FCS measurement gives $\alpha = 0.565 \pm 0.007$ and $\tau = (4.1 \pm 0.4) \times 10^{-8}$ s. The ensemble static fluorescence measurement gives $R = 0.57 \pm 0.04$. Substituting these values into eq 11 and eq 12, we find that $Q = 0.14 \pm 0.05$ and $K_d = 1.0 \pm 0.1$. Accordingly, the forward and reverse diffusion rate constants k_{d+} and k_{d-}, are $(1.2 \pm 0.2) \times 10^7$ s^{-1}, respectively.

The ultrafast measurements allow us to obtain not only the brightness of state B but also the equilibrium constant, K_d. For TMR in 19.1 mM guanosine, the amplitude of the fast component (~200 ps) and the slower component (2200 ps) should be proportional to the concentration of B and A, respectively. Thus with the parameters shown in Tables 1 and 2, we obtain that $K_d = 1.2 \pm 0.1$. Q and K_d determined from the FCS and ensemble static fluorescence data are in agreement with the femtosecond transient absorption measurements.

Interpretation of and Extraction Information from The FCS Data. Here, we showed that it is important to consider the three-state model, or the equivalent two-state model, if we wish to accurately obtain the rate constants by using PET-FCS data. If we would use a traditional two-state model, then the PET-FCS curve would reflect the relaxation between an open bright fluorescent state and a closed completely dark nonfluorescent state, and we would have $\alpha = K_d$ in eq 9. We would then derive $Q = 0$, $K_d = 0.565 \pm 0.007$, $k_{d+} = (8.8 \pm 0.7) \times 10^6$ s^{-1}, and $k_{d-} = (1.57 \pm 0.14) \times 10^7$ s^{-1}, which is quite different from the results of the equivalent two-state model ($Q = 0.14 \pm 0.05$, $K_d = 1.0 \pm 0.1$, and $k_{d+} = k_{d-} = (1.2 \pm 0.2) \times 10^7$ s^{-1}) and from that of the ultrafast experiments ($Q = 0.10 \pm 0.02$, $K_d = 1.2 \pm 0.1$, $k_{q+} = (4.1 \pm 0.8) \times 10^9$ s^{-1} and $k_{q-} = (5.2 \pm 1.0) \times 10^{10}$ s^{-1}).

Our work clearly shows that the dissociation lifetime derived from the PET-FCS experiments is the lifetime of the collision complex between the dye and the quencher instead of the lifetime of the charge separation state in the collision complex. The fact is that the lifetime of the charge separation state in the collision complex is too short to be measured by the FCS technique. The physical picture related to the PET-based experiments should be as shown in Figure 4. When the dye and the

quencher is far away, which is the bright open state A, the dye goes through the cycle of laser excitation and fluorescence emission, and the maximum rate of the cycle is limited by the fluorescence lifetime of the dye. When the dye collides with the quencher, the collision complex B is formed. Now, the laser excitation goes through two pathways, fluorescence or charge separation. In the case of TMR (probably most commonly used PET dyes, too), the lifetime of the charge separation state in the collision complex is shorter than the fluorescence lifetime, the dye after excitation goes back to the ground-state even faster than the free dye does. At the limit of weak excitation, the relative brightness of B (Q) is determined by eq 4.

The PET-FCS technique is a very powerful tool to study biomolecular processes, and we expect to see more and more its applications in the future. However, as discussed in this work, some careful consideration has to be made if we wish to extract accurate information from it. In the traditional two-state model, the PET-FCS curve alone allows one to derive the forward and reverse rate constants. However, its physical interpretation is not accurate. When more accurate physical interpretation is considered, the PET-FCS data alone are no longer sufficient to extract the forward and reverse rate constants. Here we proposed and checked two ways to gain additional information, that is, transient absorption (or fluorescence) and ensemble static fluorescence measurements. Which one is good will depend on specific situation, for which the experimental errors vary with system and equipment. Sometimes the transient data are accurate, sometimes the ensemble static fluorescence data are accurate, and sometimes they together are needed. In any cases, an appropriate choice for the reference sample (i.e., the sample of the nonquenched state only) is critical in extracting accurate K_d and Q.

CONCLUSIONS

In summary, we have investigated the PET process between TMR and guanosine in aqueous solution with femtosecond transient absorption spectroscopy. We measured the decay rate of the first excited electronic state and the recovery rate of the ground electronic state of TMR in the presence of guanosine, and we obtained the charge separation rate ($k_{q+} = (4.1 \pm 0.8) \times 10^9$ s^{-1}) and the charge recombination rate ($k_{q-} = (5.2 \pm 1.0) \times 10^{10}$ s^{-1}) in the collision complex between TMR and guanosine. On the basis of the three-state model provided by Qu et al.,[58] we suggested an equivalent two-state model, in which the dark state is composed of fluorescent and nonfluorescent states, to accurately interpret the PET-FCS data. Q and K_d determined from the PET-FCS and ensemble static fluorescence measurements are in agreement with the femtosecond transient measurements, illustrating the importance of the nonzero relative brightness of the collision complex. In addition, we found that the dissociation lifetime derived from the PET-FCS experiment is the lifetime of the collision complex between the dye and the quencher instead of the lifetime of the charge separation state in the collision complex. The lifetime of the charge separation state in the collision complex is much shorter than the lifetime of the collision complex. This work demonstrated that the PET-FCS data alone are no longer sufficient to extract the forward and reverse rate constants when more accurate physical interpretation is considered. Transient absorption, fluorescence lifetime, and fluorescence intensity measurements can provide additional necessary information.

ASSOCIATED CONTENT

Supporting Information. The fluorescence decay time profiles of TMR in different concentrations of guanosine in 1 × TE buffer obtained by time correlated single photon counting measurements, magic-angle femtosecond fluorescence up-conversion signals of TMR in 1.00 M guanosine in 1 × TE buffer, and the femtosecond transient absorption spectra on the PET process between TMR and tryptophan. This material is available free of charge via the Internet at http://pubs.acs.org.

AUTHOR INFORMATION

Corresponding Author

*Phone: +86-10-6275-1727; Fax: +86-10-6275-1708; E-mail: zhaoxs@pku.edu.cn (X.S.Z.). Phone: +86-10-6251-4601; Fax: +86-10-6251-6444; E-mail: a.yu@chem.ruc.edu.cn (A.Y.).

ACKNOWLEDGMENT

This work was supported by the National Natural Science Foundation of China (20603047, 20733001, 20973015), by the 973 Projects (2006CB910300, 2010CB912302), and by the Fundamental Research Funds for the Central Universities and the Research Funds of Renmin University of China (10XNJ008).

REFERENCES

(1) Michalet, X.; Weiss, S.; Jager, M. *Chem. Rev.* **2006**, *106*, 1785–1813.
(2) Edman, L.; Mets, U.; Rigler, R. *Proc. Natl. Acad. Sci. U.S.A.* **1996**, *93*, 6710–6715.
(3) Eggeling, C.; Fries, J. R.; Brand, L.; Gunther, R.; Seidel, C. A. M. *Proc. Natl. Acad. Sci. U.S.A.* **1998**, *95*, 1556–1561.
(4) Giepmans, B. N. G.; Adams, S. R.; Ellisman, M. H.; Tsien, R. Y. *Science* **2006**, *312*, 217–224.
(5) Piehler, J. *Curr. Opin. Struct. Biol.* **2005**, *15*, 4–14.
(6) Royer, C. A. *Chem. Rev.* **2006**, *106*, 1769–1784.
(7) Krichevsky, O.; Bonnet, G. *Rep. Prog. Phys.* **2002**, *65*, 251–297.
(8) Schuler, B.; Eaton, W. A. *Curr. Opin. Struct. Biol.* **2008**, *18*, 16–26.
(9) Lilley, D. M. J.; Wilson, T. J. *Curr. Opin. Struct. Biol.* **2000**, *4*, 507–517.
(10) Jares-Erijman, E. A.; Jovin, T. M. *Curr. Opin. Struct. Biol.* **2006**, *10*, 409–416.
(11) Selvin, P. R. *Nat. Struct. Biol.* **2000**, *7*, 730–734.
(12) Truong, K.; Ikura, M. *Curr. Opin. Struct. Biol.* **2001**, *11*, 573–578.
(13) Nettels, D.; Gopich, I. V.; Hoffmann, A.; Schuler, B. *Proc. Natl. Acad. Sci. U.S.A.* **2007**, *104*, 2655–2660.
(14) Nettels, D.; Hoffmann, A.; Schuler, B. *J. Phys. Chem. B* **2008**, *112*, 6137–6146.
(15) Kelley, S. O.; Barton, J. K. *Science* **1999**, *283*, 375–381.
(16) Kelley, S. O.; Holmlin, R. E.; Stemp, E. D. A.; Barton, J. K. *J. Am. Chem. Soc.* **1997**, *119*, 9861–9870.
(17) Lewis, F. D.; Letsinger, R. L.; Wasielewski, M. R. *Acc. Chem. Res.* **2001**, *34*, 159–170.
(18) Lewis, F. D.; Wu, T. F.; Zhang, Y. F.; Letsinger, R. L.; Greenfield, S. R.; Wasielewski, M. R. *Science* **1997**, *277*, 673–676.
(19) Meade, T. J.; Kayyem, J. F. *Angew. Chem., Int. Ed.* **1995**, *34*, 352–354.
(20) Wan, C. Z.; Fiebig, T.; Kelley, S. O.; Treadway, C. R.; Barton, J. K.; Zewail, A. H. *Proc. Natl. Acad. Sci. U.S.A.* **1999**, *96*, 6014–6019.
(21) Marme, N.; Knemeyer, J. P.; Sauer, M.; Wolfrum, J. *Bioconjugate Chem.* **2003**, *14*, 1133–1139.
(22) Neuweiler, H.; Sauer, M. *Curr. Pharm. Biotechnol.* **2004**, *5*, 285–298.

(23) Torimura, M.; Kurata, S.; Yamada, K.; Yokomaku, T.; Kamagata, Y.; Kanagawa, T.; Kurane, R. *Anal. Sci.* **2001**, *17*, 155–160.
(24) Vaiana, A. C.; Neuweiler, H.; Schulz, A.; Wolfrum, J.; Sauer, M.; Smith, J. C. *J. Am. Chem. Soc.* **2003**, *125*, 14564–14572.
(25) Marme, N.; Knemeyer, J. P.; Wolfrum, J.; Sauer, M. *Angew. Chem., Int. Ed.* **2004**, *43*, 3798–3801.
(26) Karolin, J.; Johansson, L. B. A.; Strandberg, L.; Ny, T. *J. Am. Chem. Soc.* **1994**, *116*, 7801–7806.
(27) Doose, S.; Neuweiler, H.; Sauer, M. *ChemPhysChem* **2009**, *10*, 1389–1398.
(28) Doose, S.; Neuweiler, H.; Sauer, M. *ChemPhysChem* **2005**, *6*, 2277–2285.
(29) Jean, J. M.; Hall, K. B. *Proc. Natl. Acad. Sci. U.S.A.* **2001**, *98*, 37–41.
(30) Rachofsky, E. L.; Osman, R.; Ross, J. B. A. *Biochemistry* **2001**, *40*, 946–956.
(31) Rachofsky, E. L.; Seibert, E.; Stivers, J. T.; Osman, R.; Ross, J. B. A. *Biochemistry* **2001**, *40*, 957–967.
(32) Fiebig, T.; Wan, C. Z.; Zewail, A. H. *ChemPhysChem* **2002**, *3*, 781–788.
(33) Manoharan, M.; Tivel, K. L.; Zhao, M.; Nafisi, K.; Netzel, T. L. *J. Phys. Chem.* **1995**, *99*, 17461–17472.
(34) Huber, R.; Fiebig, T.; Wagenknecht, H. A. *Chem. Commun.* **2003**, 1878–1879.
(35) Marquez, C.; Pischel, U.; Nau, W. M. *Org. Lett.* **2003**, *5*, 3911–3914.
(36) Wanninger-Weiss, C.; Valis, L.; Wagenknecht, H. A. *Bioorg. Med. Chem.* **2008**, *16*, 100–106.
(37) Seidel, C. A. M.; Schulz, A.; Sauer, M. H. M. *J. Phys. Chem.* **1996**, *100*, 5541–5553.
(38) Knemeyer, J. P.; Marme, N.; Sauer, M. *Anal. Chem.* **2000**, *72*, 3717–3724.
(39) Piestert, O.; Barsch, H.; Buschmann, V.; Heinlein, T.; Knemeyer, J. P.; Weston, K. D.; Sauer, M. *Nano Lett.* **2003**, *3*, 979–982.
(40) Heinlein, T.; Knemeyer, J. P.; Piestert, O.; Sauer, M. *J. Phys. Chem. B* **2003**, *107*, 7957–7964.
(41) Neuweiler, H.; Schulz, A.; Vaiana, A. C.; Smith, J. C.; Kaul, S.; Wolfrum, J.; Sauer, M. *Angew. Chem., Int. Ed.* **2002**, *41*, 4769–4773.
(42) Neuweiler, H.; Schulz, A.; Bohmer, M.; Enderlein, J.; Sauer, M. *J. Am. Chem. Soc.* **2003**, *125*, 5324–5330.
(43) Buschmann, V.; Weston, K. D.; Sauer, M. *Bioconjugate Chem.* **2003**, *14*, 195–204.
(44) Sauer, M.; Drexhage, K. H.; Lieberwirth, U.; Muller, R.; Nord, S.; Zander, C. *Chem. Phys. Lett.* **1998**, *284*, 153–163.
(45) Kim, J.; Doose, S.; Neuweiler, H.; Sauer, M. *Nucleic Acids Res.* **2006**, *34*, 2516–2527.
(46) Nazarenko, I.; Lowe, B.; Darfler, M.; Ikonomi, P.; Schuster, D.; Rashtchian, A. *Nucleic Acids Res.* **2002**, *30*, e37.
(47) Nazarenko, I.; Pires, R.; Lowe, B.; Obaidy, M.; Rashtchian, A. *Nucleic Acids Res.* **2002**, *30*, 2089–2095.
(48) Kurata, S.; Kanagawa, T.; Yamada, K.; Torimura, M.; Yokomaku, T.; Kamagata, Y.; Kurane, R. *Nucleic Acids Res.* **2001**, *29*, e34.
(49) McEwen, D. P.; Gee, K. R.; Kang, H. C.; Neubig, R. R. *Anal. Biochem.* **2001**, *291*, 109–117.
(50) Cunningham, C. W.; Mukhopadhyay, A.; Lushington, G. H.; Blagg, B. S. J.; Prisinzano, T. E.; Krise, J. P. *Mol. Pharm.* **2010**, *7*, 1301–1310.
(51) Kenmoku, S.; Urano, Y.; Kojima, H.; Nagano, T. *J. Am. Chem. Soc.* **2007**, *129*, 7313–7318.
(52) Wang, L.; Gaigalas, A. K.; Blasic, J.; Holden, M. J. *Spectrochim. Acta A: Mol. Bio. Spectrosc.* **2004**, *60*, 2741–2750.
(53) Johansson, M. K.; Cook, R. M. *Chem.—Eur. J.* **2003**, *9*, 3466–3471.
(54) Marras, S. A. E.; Kramer, F. R.; Tyagi, S. *Nucleic Acids Res.* **2002**, *30*, e122.
(55) Proudnikov, D.; Yuferov, V.; Zhou, Y.; LaForge, K. S.; Ho, A.; Kreek, J. K. *J. Neurosci. Method* **2003**, *123*, 31–45.
(56) Emans, N.; Biwersi, J.; Verkman, A. S. *Biophys. J.* **1995**, *69*, 716–728.
(57) Qu, P.; Chen, X. D.; Zhou, X. X.; Li, X.; Zhao, X. S. *Sci. China Ser. B: Chem.* **2009**, *52*, 1653–1659.
(58) Qu, P.; Yang, X. X.; Li, X.; Zhou, X. X.; Zhao, X. S. *J. Phys. Chem. B* **2010**, *114*, 8235–8243.
(59) Chen, X. D.; Zhou, Y.; Qu, P.; Zhao, X. S. *J. Am. Chem. Soc.* **2008**, *130*, 16947–16952.
(60) Liu, P. C.; Meng, X. L.; Qu, P.; Zhao, X. S.; Wang, C. C. *J. Phys. Chem. B* **2009**, *113*, 12030–12036.
(61) Beaumont, P. C.; Johnson, D. G.; Parsons, P. J. *J. Photochem. Photobiol. A: Chem* **1997**, *107*, 175–183.